

Preface to the Focus Section on the 6 February 2018 M_w 6.4 Hualien, Taiwan, Earthquake

by Kuo-Fong Ma and Yih-Min Wu

An intense earthquake swarm with several tens of M_w 5+ class events began shaking offshore eastern Taiwan on 4 February 2018. Two days after the swarm began, an M_L 6.26 (M_w 6.4) earthquake struck eastern Taiwan on 6 February 2018 at 11:50 p.m. (local time). This earthquake originated offshore approximately 15 km north of the city of Hualien at a depth of about 10 km and ruptured toward the southwest, with a surface rupture inland within the city of Hualien along the Milun fault. This surface rupture resulted in severe damage to several tall buildings and caused 17 deaths, as well as 289 injuries. The centroid moment tensor (CMT) focal mechanism from the Taiwan Central Weather Bureau (CWB) and the generalized Cut-and-Paste (gCAP) from the Broadband Array in Taiwan for Seismology demonstrated that this M_w 6.4 event had mainly a strike-slip focal mechanism with a minor thrust component dipping to the west. It also had a large compensated linear vector dipole (CLVD) component, consistent with the U.S. Geological Survey CMT solution and the real-time moment tensor solution (Lee *et al.*, 2013). The field investigation report of the Central Geological Survey (CGS, 2018) suggested a possible involvement of two identified surface ruptures, one along the Milun fault and another along the Linding fault, despite the origination of the mainshock offshore northeast of Hualien. However, the observed surface rupture along the Milun fault is a strike-slip fault dipping to the east. The discrepancy between the focal mechanism of the mainshock and the observed surface rupture inland along the Milun fault has focused attention on this event and also raised doubt about the rupture mechanism of the 2018 Hualien earthquake.

Historical events in this region have been studied and characterized by the features of previous earthquake swarms (Shyu, Chen, *et al.*, 2016). Significant historical damaging earthquakes occurred on 22 October 1951, when three M_w 7+ class earthquakes happened within 12 hrs. Several surface rupture patterns of the 6 February 2018 event were found to be similar to those of the 22 October 1951 events along the Milun fault. The Taiwan Earthquake Model (TEM) project published a National Seismic Hazard Map in December 2015 (Wang *et al.*, 2016) and showed that the Hualien region has about an 80% probability of experiencing an earthquake with the CWB intensity V (> 80 Gal) or larger in next 50 yrs. The seismogenic structures (Shyu, Chuang, *et al.*, 2016) that were adopted for the seismic hazard map revealed a short recurrence interval of the Milun fault of 70 yrs and thus the highest seismic potential, with a probability of an M_w 6.4 earthquake of about 42% in the next 50 yrs. Unfortunately,

this high-seismic-hazard potential did not receive enough attention at the time, resulting in significant damages and casualties during the 2018 sequence.

Seismic recordings from the CWB strong-motion network and the *P*-alert system (Wu *et al.*, 2013), an earthquake early warning (EEW) system operated by the Taiwan Earthquake Research Center, both showed that this earthquake struck inland eastern Taiwan with high intensity, yielding a peak ground acceleration (PGA) of more than 400 Gal and a pulse-like velocity motion of about 100 cm/s. The low-cost high-performance dense *P*-alert network has proven to be extremely helpful in understanding the physical generation of this strong motion, especially in relation to building damage. Exactly 2 yrs before the 6 February 2018 Hualien earthquake, the 6 February 2016 M_w 6.4 Meinong earthquake occurred in southwestern Taiwan. This earthquake also generated large pulse-like velocity motions that were responsible for much damage (Kanamori *et al.*, 2017) and that also were recorded by the dense *P*-alert network (Wu *et al.*, 2016). Lin *et al.* (2018) used the unfiltered dense *P*-alert records from the Meinong earthquake to identify the location and the slip patch on the fault plane responsible for the generation of the destructive pulse-like velocity motion. Jan *et al.* (2018) showed that the near-real-time intensity map for the Meinong earthquake derived from the *P*-alert system is helpful to identify the rupture direction and thus the identification of a mainshock rupture plane.

In the focus section on the 6 February 2018 M_w 6.4 Hualien, Taiwan, earthquake, we present 11 articles that investigate various aspects of this recent earthquake sequence. Some articles examine data from the CWB strong-motion network and the *P*-alert system, and other studies perform joint inversions of seismic and geodetic data to explain the rupture characteristics of this earthquake. Some articles also include discussions of the ground deformation based on geodetic observation, site and geotechnical investigations, examination of the aftershocks, and exploration of the possible velocity changes after the earthquake.

Wu *et al.* (2018) documented the reliable performance of the *P*-alert network and its ability to provide on-site EEW and a map of expected ground shaking within 2 min of the mainshock origin time that is in good agreement with the patterns of observed damage in the area. Lee, Lin, *et al.* (2018) mapped the spatial slip distribution of the Hualien earthquake using three fault planes, namely an offshore western dipping fault plane and two shallow faults associated with the identified

surface ruptures of the Milun and Linding faults. They concluded that a fault-to-fault jumping rupture occurred during the M_w 6.4 Hualien mainshock. Their joint-source inversion results indicated that the initial rupture started from a north-south-striking fault dipping to the west and propagated to the south with a high rupture speed, then ruptured to the shallower east-dipping Milun fault with a slower rupture speed and continued to the Linding fault in the northernmost Longitudinal Valley. [Jian et al. \(2018\)](#) used a backprojection method to image the rupture characteristics of the mainshock as well as the largest foreshock before the mainshock. The studies reveal that the foreshock ruptured northeastward and downward on a west-northwest-striking, north-northeast-dipping subhorizontal fault and that the mainshock propagated to the southwest along a north-northeast-south-southwest-striking, high-angle subvertical fault. The mainshock required a multiple point-source model that includes an M_w 6.2 and three smaller sub-events, resulting in a high CLVD component. They concluded that the 2018 Hualien earthquake sequence represents a combined consequence of ongoing concurrent oblique subduction and lateral compression beneath the northern tip of the Taiwan-Luzon arc collision zone.

As noted above, the strong-motion stations recorded pulse-like velocity motion of peak ground velocity of ~ 100 cm/s, with a period of about 1 s. These pulse-like velocity motions were considered to be responsible for the extensive damage in the city of Hualien. The pulse-like velocities were observed at all stations within a distance of 4 km from the Milun fault. [Kuo, Huang, et al. \(2018\)](#) suggested that the generation of such long-period velocity records might have resulted from the fact that the stations are located along the rupture front and are a result of site amplification. They also concluded that the soil nonlinearity resulted in a smaller horizontal PGA than vertical PGA at many stations in the near-fault region. Despite the identification of the long-period pulse-like velocity motion, geotechnical engineers also examined the possible effects of liquefaction on structural damages. [Ko et al. \(2018\)](#) investigated soil liquefaction and ground settlements during the earthquake, based on the results of a geotechnical field reconnaissance. They reported sparse liquefaction and ground settlement in the city of Hualien at the former wetland, localized in weak ground, causing no damage to structures and facilities. However, in the Hualien port, liquefaction of backfill material was found, but there was only scarcely noticeable tilt and structural damage of the caisson quay walls and scant settlement of the apron.


In addition to the comprehensive recording of ground motions, [Yen et al. \(2018\)](#) analyzed Interferometric Synthetic Aperture Radar (InSAR) and Global Positioning System (GPS) data and produced a 3D displacement model with InSAR and azimuth offset of radar images to document surface deformation after the earthquake. The 3D-displacement model was inverted to estimate slip on the Milun fault. Based on the obtained results, they proposed a model for transpressive deformation in a zone of oblique convergence and left-lateral wrench tectonics to explain this and a 22 October 1951

M_w 7.3 earthquake. [Kuo, Wang, et al. \(2018\)](#) used high-resolution Pleiades optical satellite imagery to study the distribution and magnitude of fault slip along the Milun fault surface rupture. They also used stereo Pleiades images to reveal detailed 3D surface displacements along the 8-km-long Milun fault. They found arc-tangent shapes in displacement profiles crossing the fault, suggesting a shallow east-dipping fault rupture extending 2–3 km in depth to 70–120 m below the surface. In addition to the observed GPS, [Tian et al. \(2018\)](#) used a physics-based baseline correction procedure to recover ground displacements from strong-motion recordings.

Two days after the mainshock, [Kuo-Chen et al. \(2018\)](#) deployed 70 temporary seismic stations around the city of Hualien for 12 days (8–19 February), with a station spacing of 1–5 km to investigate the locations and focal mechanisms of aftershocks and their possible tectonic implications. They located 2192 aftershocks with 580 focal mechanisms. The aftershock sequence with near-vertical distribution and a steeply west-dipping plane extended about 25 km to the southwest from the mainshock epicenter into the Longitudinal Valley and to a depth of 5–15 km. Interestingly, they found that the focal mechanisms of the aftershocks are predominantly extensional, different from the left-lateral strike slip with thrust-component faulting of the mainshock. From the mainshock to the aftershocks, the inverted horizontal stress changed rapidly from a north-northwest-oriented compressional axis (P axis) to the same direction for the extensional axis (T axis). [Lee, Chen, et al. \(2018\)](#) tried to quantify temporal variations after the mainshock using repeating aftershocks. They applied a graphic processing unit (GPU)-based template-matching algorithm (cuNCC) to discover that potential repeating earthquakes occurred before and after the 2018 M_w 6.4 Hualien earthquake. Their measurements show statistically significant delays of body waves, especially S waves of repeating aftershocks, with wave propagation paths crossing the aftershock zone of the 2018 Hualien earthquake. In addition to direct body waves, measurements at some stations show significant delays for P and S coda waves.

To examine the performance of the TEM's probabilistic seismic hazard analysis (PSHA) 2015 model PSHA2015, [Chan et al. \(2018\)](#) considered a retrospective forecast of the seismic activities of the 2018 Hualien sequence, with recommendations for the next generation of seismic hazard assessment for Taiwan. They confirmed the model credibility of the area sources by comparing the locations of the Hualien sequence and seismicity during the period from 2012 to 2016. They also concluded similar forecasting reliability for the smoothing model, which could be incorporated in the next generation of PSHA as a branch of the logic tree. The TEM PSHA2015 model forecasts the rupture probability as 53% within 50 yrs, and the Brownian passage time (BPT) model forecasts the rupture probability as 80% for the next 50 yrs. The BPT model, which also considers time-dependency rupture probability, is suggested for future hazard assessment, especially for the seismogenic-structure sources with records of their recent ruptures. They conclude that this earthquake sequence highlights the

importance of short-term seismic hazard assessment that provides a basis for rapid response after a devastating earthquake.

In summary, the first three articles in this *SRL* focus section report the rupture pattern of the Hualien mainshock, based on information from a dense *P*-alert network, joint inversion, and backprojection. Two subsequent articles discuss the site and geotechnical aspects of the observed damage and ground failures. The next three studies on ground deformation used geodetic data to reveal the seismotectonic structure and a technique on the integration of the strong-motion data. The ninth article captures the behavior of the aftershocks by reporting on the quick deployment of a dense seismic array, which made it possible to observe the change of the aftershock stress axis from the mainshock stress axis. The 10th article shows the efficient development in detecting the velocity changes from repeating aftershocks using GPU computation. The 11th paper confirms the reliability of the developed seismic hazard map and presents suggestions for the time-dependent analysis on seismic hazard probability. Together, these articles provide first-hand information about the rupture characteristics, fault mechanism, and damage patterns associated with the 6 February 2018 M_w 6.4 Hualien, Taiwan, earthquake. These studies also highlight the importance of developing a reliable seismic hazard map in seismically active regions, increasing station coverage to capture the mainshock rupture, open sharing of geophysical data, and rapid postmainshock field survey and seismic deployment to quantify damages and capture aftershocks. 

ACKNOWLEDGMENTS

The guest editors would like to thank all the authors for their timely contributions and all the reviewers for their careful and constructive comments. The authors also thank *SRL* Editor-in-Chief Zhigang Peng for inviting us to be the guest editors of this focus section and *SRL* Managing Editor Mary George for her assistance.

REFERENCES

- Central Geological Survey (2018). Preliminary geological survey of the 2018 Hualien earthquake, available at <https://www.moeacgs.gov.tw/info/view.jsp?info=983> (last accessed November 2018) (in Chinese).
- Chan, C. H., K. F. Ma, Y. T. Lee, and Y. J. Wang (2018). Rethinking seismic source model of probabilistic hazard assessment in Taiwan after the 2018 Hualien, Taiwan, earthquake sequence, *Seismol. Res. Lett.* doi: [10.1785/0220180225](https://doi.org/10.1785/0220180225).
- Jan, J.-C., H. H. Huang, Y. M. Wu, C. C. Chen, and C. H. Lin (2018). Near-real-time estimates on earthquake rupture directivity using near-field ground motion data from a dense low-cost seismic network, *Geophys. Res. Lett.* **45**, 7496–7503, doi: [10.1029/2018GL078262](https://doi.org/10.1029/2018GL078262).
- Jian, P. R., S. H. Hung, and L. Meng (2018). Rupture behavior and interaction of the 2018 Hualien earthquake sequence and its tectonic implication, *Seismol. Res. Lett.* doi: [10.1785/0220180241](https://doi.org/10.1785/0220180241) (this issue).
- Kanamori, H., L. Ye, B. S. Huang, H. H. Huang, S. J. Lee, W. T. Liang, Y. Y. Lin, K. F. Ma, Y. M. Wu, and T. Y. Yeh (2017). A strong-motion hot spot of the 2016 Meinong, Taiwan, earthquake ($M_w = 6.4$), *Terr. Atmos. Ocean. Sci.* **28**, 637–650, doi: [10.3319/TAO.2016.10.07.01](https://doi.org/10.3319/TAO.2016.10.07.01).
- Ko, Y. Y., S. Y. Hsu, H. C. Yang, C. C. Lu, Y. W. Hwang, C. H. Liu, and J. H. Hwang (2018). Soil liquefaction and ground settlements in 6 February 2018 Hualien, Taiwan, earthquake, *Seismol. Res. Lett.* doi: [10.1785/0220180196](https://doi.org/10.1785/0220180196).
- Kuo, C. H., J. Y. Huang, C. M. Lin, T. Y. Hsu, S. H. Chao, and K. L. Wen (2018). Strong ground motion and pulse-like velocity observations in the near-fault region of the 2018 M_w 6.4 Hualien, Taiwan, earthquake, *Seismol. Res. Lett.* doi: [10.1785/0220180195](https://doi.org/10.1785/0220180195).
- Kuo, Y. T., Y. Wang, J. Hollingsworth, S. Y. Huang, R. Y. Chuang, C. H. Lu, Y. C. Hsu, H. Tung, J. Y. Yen, and C. P. Chang (2018). Shallow fault rupture of the Milun fault in the 2018 M_w 6.4 Hualien earthquake: A high-resolution approach from optical correlation of Pléiades satellite imagery, *Seismol. Res. Lett.* doi: [10.1785/0220180227](https://doi.org/10.1785/0220180227) (this issue).
- Kuo-Chen, H., Z. K. Guan, W. F. Sun, P. Y. Jhong, and D. Brown (2018). Aftershock sequence of the 2018 M_w 6.4 Hualien earthquake in eastern Taiwan from a dense seismic array data set, *Seismol. Res. Lett.* doi: [10.1785/0220180233](https://doi.org/10.1785/0220180233).
- Lee, E.-J., P. Chen, D. Mu, R. J. Rau, and C. M. Lin (2018). Coseismic velocity variations associated with the 2018 M_w 6.4 Hualien earthquake estimated using repeating earthquakes, *Seismol. Res. Lett.* doi: [10.1785/0220180230](https://doi.org/10.1785/0220180230) (this issue).
- Lee, S.-J., W. T. Liang, H. W. Cheng, F. S. Tu, K. F. Ma, H. Tsuruoka, H. Kawakatsua, B. S. Huang, and C. C. Liu (2013). Toward real-time regional earthquake simulation. I: Real-time moment tensor monitoring (RMT) for regional events in Taiwan, *Geophys. J. Int.* **87**, 56–68.
- Lee, S.-J., T. C. Lin, T. Y. Liu, and T. P. Wong (2018). Fault-to-fault jumping rupture of the 2018 M_w 6.4 Hualien earthquake in eastern Taiwan, *Seismol. Res. Lett.* doi: [10.1785/0220180182](https://doi.org/10.1785/0220180182).
- Lin, Y. Y., T. Y. Yeh, K. F. Ma, T. R. A. Song, S. J. Lee, B. S. Huang, and Y. M. Wu (2018). Source characteristics of the 2016 Meinong (M_L 6.6), Taiwan, earthquake, revealed from dense seismic arrays: Double sources and pulse-like velocity ground motion, *Bull. Seismol. Soc. Am.* **108**, 188–199, doi: [10.1785/0120170169](https://doi.org/10.1785/0120170169).
- Shyu, J. B. H., C.-F. Chen, and Y.-M. Wu (2016). Seismotectonic characteristics of the northernmost Longitudinal Valley, eastern Taiwan: Structural development of a vanishing suture, *Tectonophysics* **692**, 295–308, doi: [10.1016/j.tecto.2015.12.026](https://doi.org/10.1016/j.tecto.2015.12.026).
- Shyu, J. B. H., Y. R. Chuang, Y. L. Chen, Y. R. Lee, and C. T. Cheng (2016). A new on-land seismogenic structure source database from the Taiwan Earthquake Model (TEM) project for seismic hazard analysis of Taiwan, *Terr. Atmos. Ocean. Sci.* **27**, 311–323, doi: [10.3319/TAO.2015.11.27.02\(TEM\)](https://doi.org/10.3319/TAO.2015.11.27.02(TEM)).
- Tian, S., P. Gardoni, and W. Yuan (2018). Coseismic deformation of the 6 February 2018 M_w 6.2 Hualien earthquake based on strong-motion recordings, *Seismol. Res. Lett.* doi: [10.1785/0220180235](https://doi.org/10.1785/0220180235) (this issue).
- Wang, Y.-J., C.-H. Chan, Y.-T. Lee, K.-F. Ma, J. B. H. Shyu, R.-J. Rau, and C.-T. Cheng (2016). Probabilistic seismic hazard assessments for Taiwan, *Terr. Atmos. Ocean. Sci.* **27**, 325–340.
- Wu, Y. M., D. Y. Chen, T. L. Lin, C. Y. Hsieh, T. L. Chin, W. Y. Chang, W. S. Li, and S. H. Ker (2013). A high density seismic network for earthquake early warning in Taiwan based on low cost sensors, *Seismol. Res. Lett.* **84**, 1048–1054, doi: [10.1785/0220130085](https://doi.org/10.1785/0220130085).
- Wu, Y. M., W. T. Liang, H. Mittal, W. A. Chao, C. H. Lin, B. S. Huang, and C. M. Lin (2016). Performance of a low-cost earthquake early warning system (P-alert) during the 2016 M_L 6.4 Meinong (Taiwan) earthquake, *Seismol. Res. Lett.* **87**, 1050–1059, doi: [10.1785/0220160058](https://doi.org/10.1785/0220160058).
- Wu, Y. M., H. Mittal, T. C. Huang, B. M. Yang, J. C. Jan, and S. K. Chen (2018). Performance of a low-cost earthquake early warning system (P-alert) and shake map production during the 2018 M_w 6.4

Hualien, Taiwan, earthquake, *Seismol. Res. Lett.* doi: [10.1785/0220180170](https://doi.org/10.1785/0220180170).

Yen, J. Y., C. H. Lu, R. J. Dorsey, H. Kuo-Chen, C. P. Chang, C. C. Wang, Y. Ray, Y. Chung, T. Kuo, C. Y. Chiu, *et al.* (2018). Insights into seismogenic deformation during the 2018 Hualien, Taiwan, earthquake sequence from InSAR, GPS, and modeling, *Seismol. Res. Lett.* doi: [10.1785/0220180228](https://doi.org/10.1785/0220180228).

Kuo-Fong Ma^{1,2}

*Earthquake-Disaster and Risk Evaluation and Management
(E-DREaM) Center
National Central University
No. 300, Chungda Road
Chungli 32054, Taiwan, Republic of China
fong@ncu.edu.tw*

Yih-Min Wu^{2,3}

*Department of Geosciences
National Taiwan University
No. 1, Section 4, Roosevelt Road
Taipei 10617, Taiwan, Republic of China
drymwu@ntu.edu.tw*

Published Online 12 December 2018

¹ Also at Department of Earth Sciences, National Central University, Taiwan.

² Also at Institute of Earth Sciences, Academia Sinica, Taipei 11529, Taiwan.

³ Also at NTU Research Center for Future Earth, National Taiwan University, Taipei 10617, Taiwan.